



Effect of Preparation Method on the Structure and Catalytic Performance of CuZnO Catalyst for Low Temperature Syngas Hydrogenation in Liquid Phase

Huan Liu^{1,2} · Tong Chen¹ · Gongying Wang¹

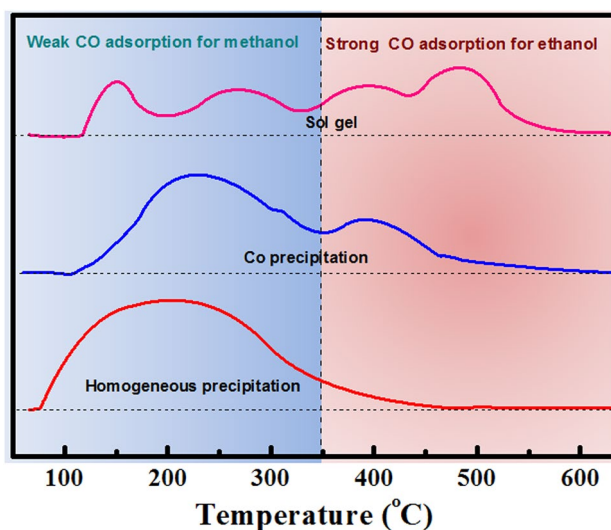
Received: 17 November 2017 / Accepted: 5 February 2018
© Springer Science+Business Media, LLC, part of Springer Nature 2018

Abstract

CuZnO catalysts were prepared by different methods, characterized by applying a combination of techniques, and the effect of preparation method on the structure and the catalytic performance for syngas hydrogenation at low temperature in liquid phase was investigated. The results showed that due to the difference of the interaction between Cu and Zn, the preparation method greatly affected the crystallinity of CuZnO. The crystallinity of CuZnO had a direct relation with the CO adsorption property. The total CO adsorption amount determined the catalytic activity, the weak adsorption of CO accounted for the methanol synthesis, while the strong adsorption of CO accounted for the ethanol synthesis. CuZnO prepared by the homogeneous precipitation with the lowest crystallinity exhibited the highest total carbon conversion of 68.6% with the methanol selectivity of 84.9%, while CuZnO prepared by the sol gel with the highest crystallinity exhibited the highest ethanol selectivity of 47.6%.

Graphical Abstract

The preparation method of CuZnO had a significant effect on the CO adsorption property and then resulted in a substantial modification in the product distribution for the syngas hydrogenation at low temperature in liquid phase. The catalytic activity was determined by the total amount of CO adsorption, the weak CO adsorption accounted for the methanol synthesis and the strong CO adsorption accounted for the ethanol synthesis.



Keywords CuZnO · Ethanol · Methanol · Preparation method · Syngas hydrogenation

Extended author information available on the last page of the article

Published online: 02 March 2018

1 Introduction

Syngas derived from coal, biomass or nature gas was widely used to produce methanol. However, higher alcohols are more desirable products than methanol as neat fuels, a potential source of hydrogen for fuel cells and a feedstock for the synthesis of variety of chemicals [1–6]. Considering the energy shortage and the deterioration of global climate change, the synthesis of higher alcohols from syngas has attracted much attention [7, 8].

Currently, the synthesis of higher alcohols synthesis from syngas was widely studied via the fixed bed reactor under high temperature and high pressure (250–440 °C and 4.1–10.3 MPa) over the modified methanol synthesis catalysts and the modified Fisher–Tropsch catalysts [1, 7, 9–15]. In order to enhance the carbon conversion and address thermodynamic limitation of syngas hydrogenation to alcohols in conventional process, the process of a low temperature syngas hydrogenation in liquid phase was developed [16–24]. For the low temperature process in liquid phase, the catalytic system with Cu based catalyst and alcohol as solvent has been widely investigated [20, 23–33]. Zn as an effective promoter could not only stabilize the active phase and also alter the interaction between components of the catalyst [34–40]. Thus, CuZnO catalyst shows good catalytic performance for the low temperature syngas hydrogenation reaction in liquid phase, but methanol was the major alcohol product [41, 42]. Previous studies about CuCo based catalyst indicated that the preparation method greatly affected the structure and then significantly influenced the catalytic activity for CO hydrogenation in the conventional process [43, 44]. However, few literatures reported the effect of the structure of CuZnO catalyst on the product distribution and catalytic activity for the low temperature syngas hydrogenation reaction in liquid phase. Furthermore, the structure played an important role in the selective synthesis of product.

In this work, CuZnO samples with different structures were prepared by different methods and characterized by XPS, H₂-TPR, XRD, SEM, TEM and CO-TPD. The relationship between the structure and the catalytic performance for the syngas hydrogenation at low temperature in liquid phase was investigated.

2 Experimental Section

2.1 Materials

Cu(NO₃)₂·3H₂O, Zn(NO₃)₂·6H₂O, K₂CO₃, Na₂CO₃, urea and citric acid were of A. R. grade. All of materials were used without further purification.

2.2 Catalyst Preparation

CuZnO samples (Cu/Zn = 1, molar ratio) with different structures were synthesized via homogeneous precipitation, conventional co precipitation and sol gel, and named as CuZnO-1, CuZnO-2 and CuZnO-3, respectively.

In the homogeneous precipitation method, an aqueous solution of copper and zinc nitrates was mixed with urea. The urea was hydrolyzed by heating the mixture to 90 °C for 24 h to release the precipitant agent (hydroxide ions). The precipitate was washed several times with deionized water and dried at 120 °C for 12 h. Finally, the sample were calcined at 350 °C for 3 h.

In the conventional co precipitation method, 100 ml mixed aqueous solution containing copper and zinc nitrates (total metal concentration of 1.0 mol/l) and an aqueous solution of Na₂CO₃ (1.0 mol/l) used as a precipitant were simultaneously added to an amount of distilled water under rapid stirring to generate precipitate. The temperature and pH of the precipitation were controlled at 65 °C and 8.5, respectively. The obtained precipitation was aged at 65 °C for 4 h, followed by filtering and washing several times with distilled water to remove residual sodium. Then, the precipitation was dried at 120 °C overnight and then calcined at 350 °C for 3 h.

In the sol gel method, an aqueous solution of copper and zinc nitrates was made to the desired composition. Then, the citric acid solution was slowly added to the metal nitrate solution under constant stirring. The resulting solution was heated at 80 °C in a water bath to evaporate excess water and a viscous gel was obtained. The gel was put into an oven at 100 °C and started boiling with frothing and foaming. Subsequently, the precursor was put in a muffle furnace, heating to 350 °C at 1 °C/min and holding at 350 °C for 3 h and form a black powder.

2.3 Catalytic Activity Test

The catalytic activity test was performed in a batch reactor with an inner volume of 100 ml. Prior to the catalytic activity test, the metallic oxide precursors of samples were reduced at 250 °C for 8 h by a flow of 10% hydrogen in nitrogen. After reduction and cooling down to room temperature, the sample was first added into the reactor with K₂CO₃ and 2-propanol. After the tightness of reactor was checked by N₂, the feed gas (H₂/CO/CO₂ = 65/33/2) was introduced to purge the inside gas. The test was conducted at 5.0 MPa and 170 °C, respectively. In case of the occurrence of the diffusion-controlled regime between gas, liquid and solid phases, the stir speed of the reactor was carefully checked and set at 1500 rpm. Liquid products were analyzed by SHIMADZU GC-14B with capillary column via internal standard method,

and gas products were analyzed by SC-3000B with packed column via external standard method.

The catalytic performance was evaluated by total carbon conversion, the selectivity of products, which were calculated as follows:

$$\text{Total carbon conversion} = \text{CO conversion} \times \frac{V_a}{V_a + V_b} + \text{CO}_2 \text{ conversion} \times \frac{V_b}{V_a + V_b}$$

where V_a and V_b represented the volume concentration of CO and CO_2 in the feed gas, respectively.

$$\text{Pi selectivity} = \frac{\text{the mole number of carbon in Pi}}{\text{the mole number of carbon converted}} \times 100\%$$

where Pi was one of the products.

3 Results and Discussion

3.1 Catalyst Characterization

The XPS spectra of CuZnO samples prepared by different methods at Cu 2p, Zn 2p and O 1s were shown in Fig. 1. It can be seen from Fig. 1 that all samples exhibited the same binding energies of Cu 2p, Zn 2p and O 1s. For Cu 2p spectra, the binding energies of Cu $2p_{1/2}$ of ~953.6 eV and Cu

$2p_{3/2}$ of ~933.6 eV attributed to Cu^{2+} were detected [45, 46]. The peaks at the binding energies of ~962.5 and ~942.5 eV were the satellite structures of Cu^{2+} , which was due to the shake-up transitions by ligand-to-metal 3d charge transfer in the form of Cu^{2+} with the $3d^9$ configuration [47, 48]. The

binding energies of Zn 2p of Zn $2p_{1/2}$ of ~1044.7 eV and Zn $2p_{3/2}$ of ~1021.7 eV attributed to Zn^{2+} were observed [49]. For O 1s spectra, the binding energy of O 1s of ~530.0 eV was ascribed to the metal oxide of CuO and ZnO, and the binding energy of O 1s of ~531.7 eV was caused by the surface hydration [5]. Apparently, the peaks of Cu 2p and Zn 2p of $2p_{1/2}$ and $2p_{3/2}$ of CuZnO-3 shifted towards lower binding energy by 0.6 eV, in contrast with that of CuZnO-1 and CuZnO-2. These results suggested that the preparation method had no effect on the chemical valence states of Cu, Zn and O, but affected the chemical environment of Cu and Zn, which led to the difference of the interaction between Cu and Zn. Thus, it was deduced that the interaction between Cu and Zn in CuZnO-1 and CuZnO-2 was stronger than that of CuZnO-3.

The H_2 -TPR profiles of CuZnO samples prepared by various methods were displayed in Fig. 2. Since ZnO could

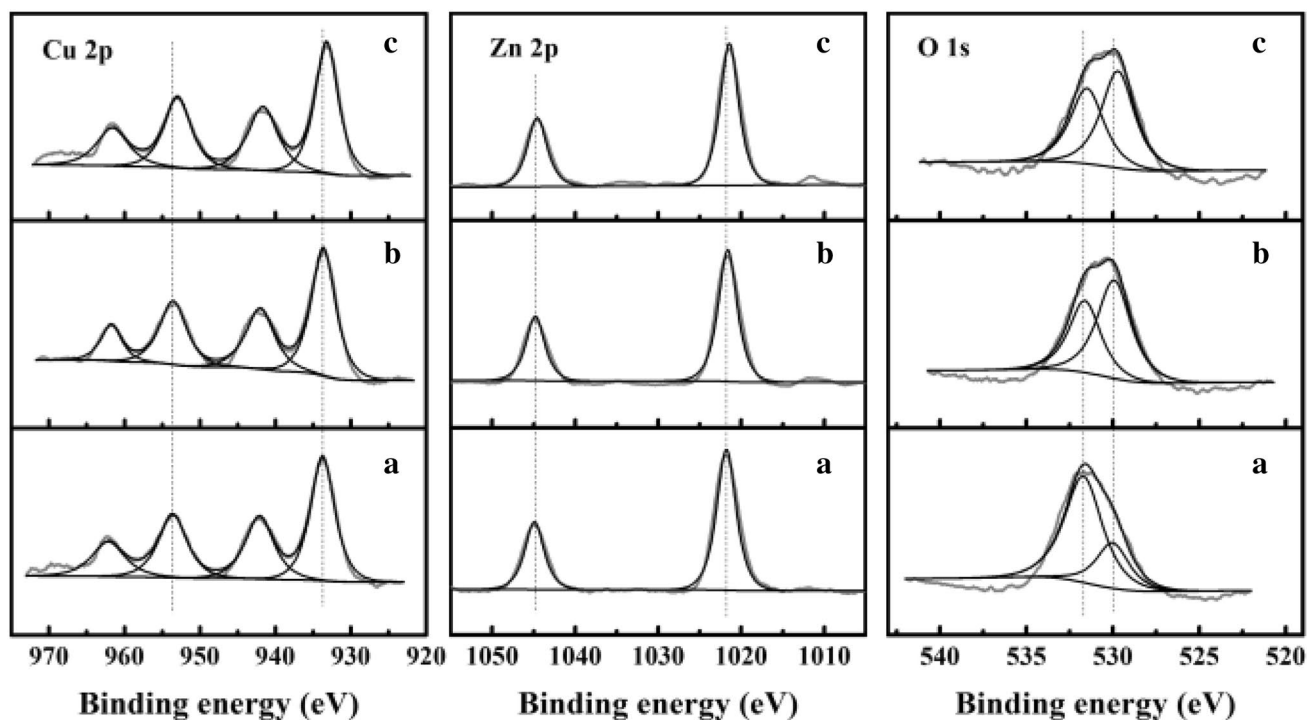


Fig. 1 The XPS spectra of CuZnO samples prepared by different methods. (a) CuZnO-1, (b) CuZnO-2, (c) CuZnO-3

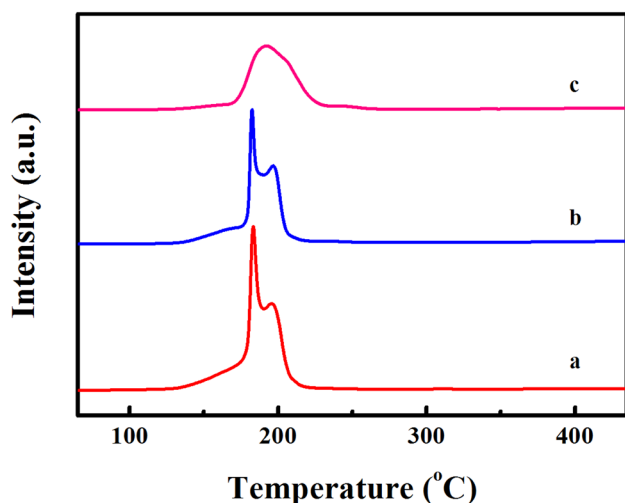


Fig. 2 The H₂-TPR profiles of CuZnO samples prepared by different methods. (a) CuZnO-1, (b) CuZnO-2, (c) CuZnO-3

Table 1 The textural properties of CuZnO samples prepared by different methods

Samples	BET surface area (m ² /g)	Pore volume (cm ³ /g)	Average pore diameter (nm)
CuZnO-1	53.7	0.26	19.68
CuZnO-2	48.4	0.25	21.31
CuZnO-3	16.4	0.07	17.26

not be reduced below 700 °C, all the reduction peaks in Fig. 2 were attributed to the reduction of copper species [50, 51]. The H₂-TPR profiles of CuZnO-1 and CuZnO-2 showed similar reduction peaks, the low temperature reduction peak at around 183 °C corresponding to the reduction of high dispersed copper species and the high temperature reduction peak at around 196 °C corresponding to the reduction of copper species interacted with zinc species [52]. The H₂-TPR profile of CuZnO-3 displayed only a broad reduction peak at around 191 °C [8, 53]. Thus, it can be deduced that comparing with the sol gel method, the precipitation method was in favor of the enhancement of the interaction between Cu and Zn, which was consistent with the result of XPS.

The BET surface area, pore volume and average pore diameter of CuZnO samples prepared by different methods were summarized in Table 1. It can be found that the preparation methods significantly affected the textural properties of CuZnO samples. For CuZnO-1, the BET surface area, pore volume and average pore diameter were 53.7 m²/g and 0.26 cm³/g with mean pore diameter of 19.68 nm, which was calculated from the pore distribution evaluated from the desorption branch by BJH method (Fig. 3). For CuZnO-2,

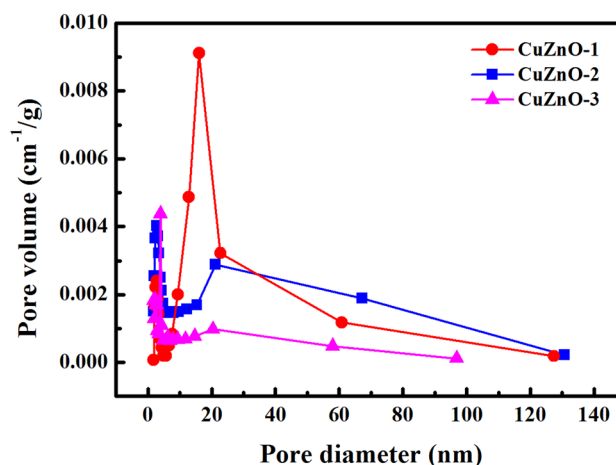


Fig. 3 The pore size distribution of CuZnO samples prepared by different methods

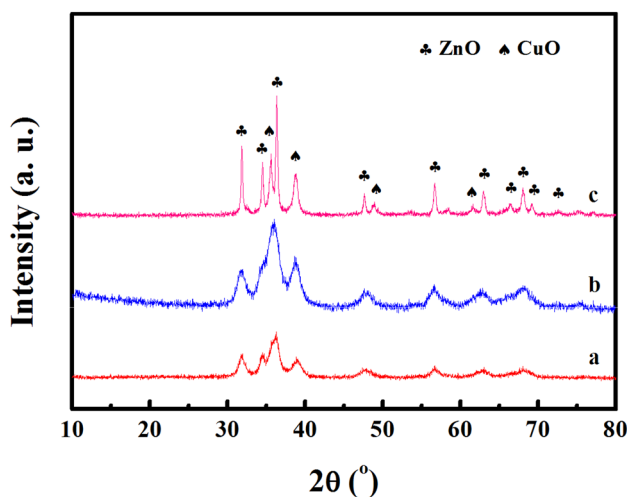


Fig. 4 The XRD patterns of CuZnO samples prepared by different methods. (a) CuZnO-1, (b) CuZnO-2, (c) CuZnO-3

the pore volume and average pore diameter were similar to that of CuZnO-1, while the BET surface area was smaller than that of CuZnO-1 by 9.8%. For CuZnO-3, the BET surface area, pore volume and average pore diameter were 16.4 m²/g, 0.07 cm³/g and 17.26 nm, which were the lower than that of two other samples. All the average pore diameter of the samples was in the range of 2–50 nm, which owned to the type of mesoporous. The results suggested that the large surface area and pore volume may provide plenty of active site and favor adsorption and diffusion of reactant gas.

The XRD patterns of CuZnO samples prepared by different methods were illustrated in Fig. 4. The characteristic peaks of CuO and ZnO were observed from the XRD patterns of the three samples. The intensities of the diffraction

peaks of CuO and ZnO phases of CuZnO samples were in the order of CuZnO-3 > CuZnO-2 > CuZnO-1. Among the three CuZnO samples, CuZnO-3 showed the highest crystallinity, that is, CuZnO-3 owned the largest particle size. Combined with the results of H₂-TPR, this result suggested that the strong interaction between Cu and Zn in CuZnO-1 and CuZnO-2 inhibited the crystal particle growth. These results suggested that the sol gel method was beneficial to the growth of the crystal particle of CuO and ZnO.

The morphologies of CuZnO samples prepared by different methods were analyzed by SEM and showed in Fig. 5. CuZnO-1 displayed fluffy plate-like crystals, which may provide high surface area for active sites and favored the adsorption and diffusion of reactant molecular, while CuZnO-2 exhibited the spongy morphology and relatively uniform sphere-like particles, which could enhance the syngas adsorption and diffusion. CuZnO-3 also showed the spongy morphology, but the particle size was larger than

that of CuZnO-2. Additionally, some agglomeration was observed in Fig. 5c, which may be caused by the local high temperature during the preparation process. The order of the crystal size of the samples prepared by different method was CuZnO-3 > CuZnO-2 > CuZnO-1. The results above were in agreement with the BET surface area of Table 1 and the analyses of XRD.

The transmission electron microscopy was used to investigate the exposed facets of CuZnO samples prepared by different methods, and the TEM images were shown in Fig. 6. The low resolution TEM images of CuZnO samples in Fig. 6a, c and e displayed that the morphology of crystals of CuZnO-1 was plate-like, the particles of CuZnO-2 were approximately spherical in shape with the size of about 8.3 nm, and the particle shape of CuZnO-3 was a mixture of sphere and plate-like crystals with the size in the range of 18–89 nm. The results were consistent with the analyses of XRD and SEM.

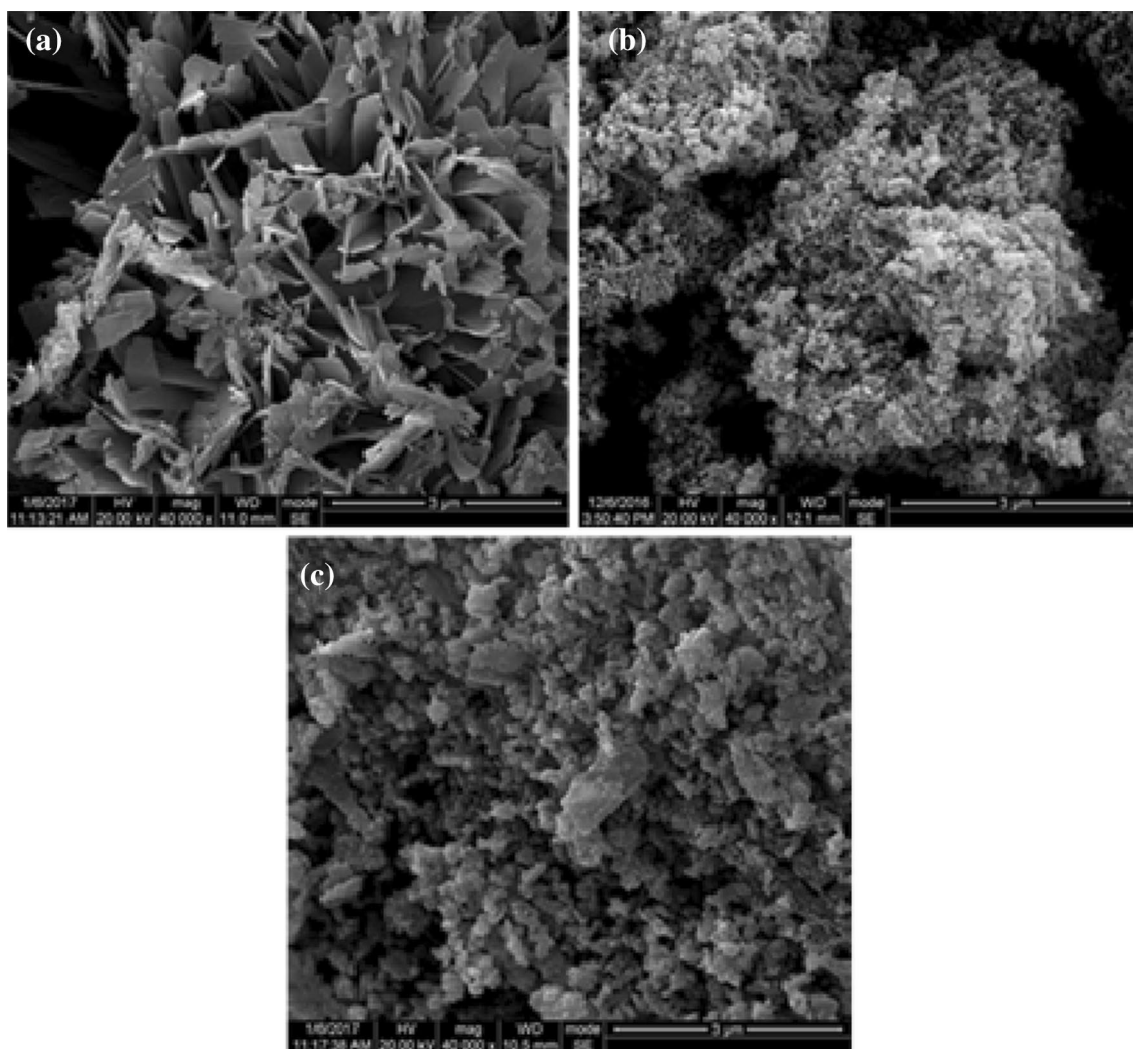


Fig. 5 The SEM images of the fresh CuZnO samples prepared by different methods. **a** CuZnO-1, **b** CuZnO-2, **c** CuZnO-3

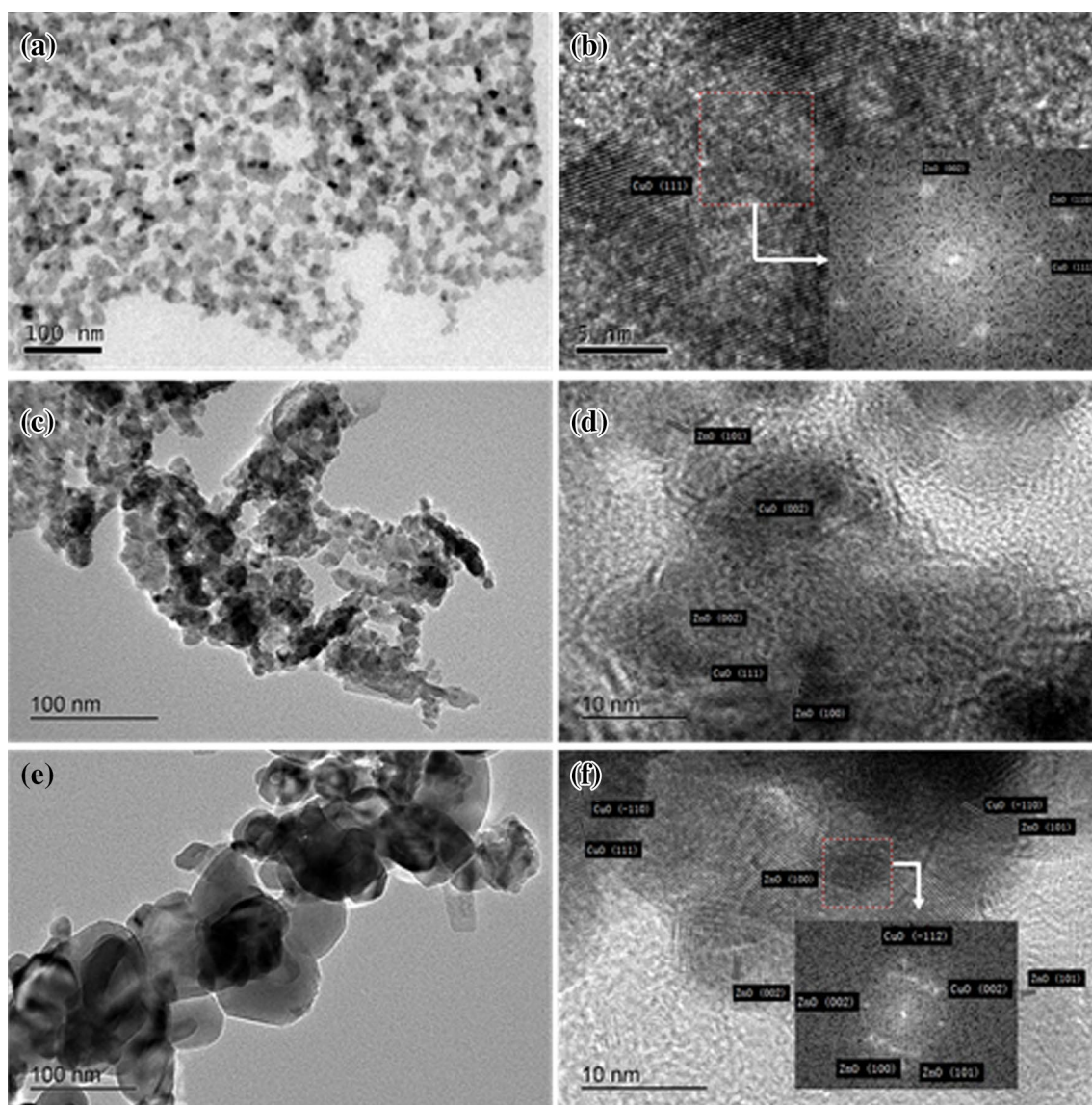


Fig. 6 The TEM images of the fresh CuZnO samples prepared by different methods. Low resolution TEM images of **a** CuZnO-1, **c** CuZnO-2, **e** CuZnO-3; High resolution TEM images of **b** CuZnO-1, **d** CuZnO-2, **f** CuZnO-3

The high resolution TEM images of three CuZnO samples were presented in Fig. 6b, d and f. The observation of the exposed facets of CuO and ZnO in the three CuZnO samples demonstrated the polycrystalline nature. CuZnO-1 mainly exhibited the facets of CuO of (1 1 1) and ZnO of (0 0 2), (1 1 0). CuZnO-2 displayed the facets of CuO of (0 0 2), (1 1 1), (−1 1 0), ZnO of (0 0 2), (1 0 1), (1 0 0) and CuZn of (3 1 0). Figure 6d of CuZnO-2 exposing much more planes of CuO and ZnO than that of CuZnO-1 indicated the higher crystallinity of CuZnO-2 than that of CuZnO-1. Figure 6f of CuZnO-3 was fully covered by the facets of CuO and ZnO, and besides the planes in Fig. 6b and d, CuO (−1 1 1) was detected, which demonstrated the highest crystallinity of CuZnO-3.

It was noteworthy that the presence of CuZn plane in CuZnO-2 suggested the existence of the interaction between Cu and Zn, which was also confirmed by H_2 -TPR. Due to the similar reducibility of CuZnO-1 and CuZnO-2, the interaction between Cu and Zn would also exist in CuZnO-1, but no CuZn facet was observed in Fig. 6b, which may own to the low crystallinity of CuZnO-1. However, no facet of CuZn was distinguishable in Fig. 6f of CuZnO-3 with the highest crystallinity, which implied that the interaction between Cu and Zn in CuZnO-3 was weak.

The CO-TPD curves of CuZnO samples prepared by different methods were shown in Fig. 7. The CO-TPD profile of CuZnO-1 displayed a broad desorption peak in the range of 70–400 °C. For CuZnO-2, two desorption peaks in the

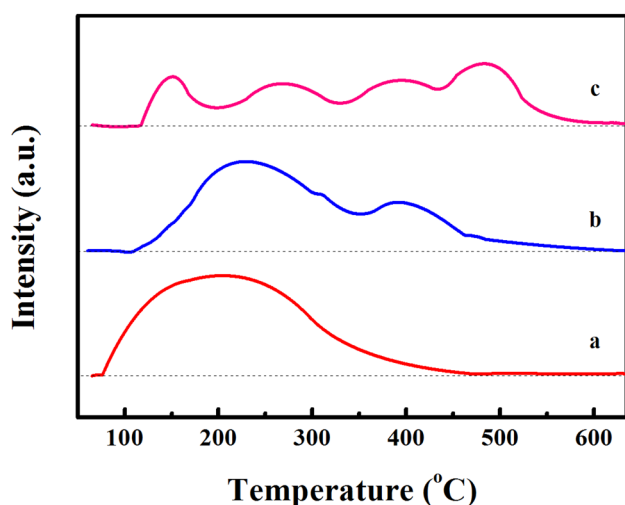


Fig. 7 The CO-TPD curves of CuZnO samples prepared by different methods. (a) CuZnO-1, (b) CuZnO-2, (c) CuZnO-3

range of 100–450 °C were identified. The CO-TPD profile of CuZnO-3 exhibited four overlapped desorption peaks in the range of 115–550 °C.

The CO desorption peak below 350 °C was regarded as the low temperature desorption peak corresponding to the weak CO adsorption, and the CO desorption peak above 350 °C was regarded as the high temperature desorption peak corresponding to the strong CO adsorption. For CuZnO-1, only the low temperature desorption peak was observed. For CuZnO-2, the amount of CO desorption at low temperature was much larger than that of CO desorption at high temperature. For CuZnO-3, the amount of CO desorption at high temperature was larger than that of CO desorption at low temperature.

Comparing the CO desorption peak area with the same sample loading, the difference of the area of the CO desorption peak in different temperature regions of the three samples was obvious. The order of the total area of CO desorption peaks was CuZnO-1 > CuZnO-2 > CuZnO-3, the order of the area of the low temperature CO desorption peak was CuZnO-1 > CuZnO-2 > CuZnO-3, and the order of the area of the high temperature CO desorption peak was CuZnO-3 > CuZnO-2 > CuZnO-1, respectively.

Combined with the analyses of XRD, it was found that the beginning CO desorption temperature and the area of the high temperature CO desorption peak were linearly related with the crystallinity of CuZnO, which suggested that high crystallinity strengthened the bond between CO and Cu, and shifted some weak CO adsorption to the strong CO adsorption.

Thus, the preparation method of CuZnO affected the interaction between copper and zinc, which resulted in the difference of the crystallinity of CuZnO samples. The

Table 2 The effect of preparation method of CuZnO on the catalytic activity and the product distribution for the low temperature conversion of syngas to ethanol in liquid phase

Samples	Total carbon conversion (%)	Selectivity (%)			
		Methanol	Ethanol	Methyl acetate	Iso-propyl formate
CuZnO-1	68.6	84.9	0	2.0	13.0
CuZnO-2	64.2	70.5	13.8	9.6	5.7
CuZnO-3	35.3	22.7	47.6	14.0	11.5

Reaction conditions: T = 170 °C, P = 5.0 MPa, H₂/CO/CO₂ = 65/33/2; 2-propanol, 30 ml; sample, 2.0 g; K₂CO₃, 0.6 g; reaction time, 10 h

precipitation method strengthened the interaction between Cu and Zn and inhibited the crystal particle growth, while the sol gel method weakened the interaction and promoted the crystal particle growth. Meanwhile, the difference of CuZnO crystallization led to a substantial modification in the CO adsorption property.

3.2 Catalytic Performance

The effect of the preparation method on catalytic performance of CuZnO sample for the low temperature ethanol synthesis from syngas in liquid phase was listed in Table 2. As expected, the preparation method had a significant effect on the catalytic activity and the product distribution. CuZnO-1 exhibited the total carbon conversion of 68.6% and the methanol selectivity of 84.9%, and methanol was the only alcohol product. CuZnO-2 exhibited the total carbon conversion of 64.2%, but ethanol was detected in the product with the selectivity of 13.8%, and the methanol selectivity decreased to 70.5%. In comparison with CuZnO-1 and CuZnO-2, the total carbon conversion over CuZnO-3 obviously decreased to 35.3%, but the selectivity towards ethanol greatly increased to 47.6% with the selectivity of methanol decreasing to 22.7%. Apparently, ethanol was synthesized at the consumption of methanol, which may be due to that the intermediate for the formation of methanol and ethanol was same.

Based on the results of CO-TPD, it was found that the total carbon conversion was associated with the total amount of CO adsorption, the selectivity of methanol was linearly related with the amount of the weak CO adsorption, and the selectivity of ethanol was linearly related with the amount of the strong CO adsorption. The results indicated that the amount of CO adsorbed over the surface determined the catalytic activity for the syngas hydrogenation, the weak adsorption of CO accounted for the product of methanol, while the strong adsorption of CO accounted for the product of ethanol. That is, the stronger bond between CO and Cu

was beneficial to the carbon chain growth to promote the ethanol synthesis.

Additionally, the catalytic activities of CuZnO-1 and CuZnO-2 were much higher than that of CuZnO-3, while the selectivity of ethanol of CuZnO-1 and CuZnO-2 were much lower than that of CuZnO-3. Two factors may be responsible for the phenomenon. First, the BET surface area of CuZnO-1 and CuZnO-2 were much larger than that of CuZnO-3, which provided much more active sites for the adsorption and diffusion of the reactant gas and then promoted the conversion of syngas, which was also confirmed by CO-TPD and SEM. Second, the strong interaction between Cu and Zn in CuZnO-1 and CuZnO-2 samples created additional new Cu-Zn bimetallic active sites for the syngas hydrogenation [40, 54, 55]. Meanwhile, the strong interaction between Cu and Zn inhibited the growth of crystal particle and decreased the amount of the strong CO adsorption, which led to the obvious decrease of the ethanol selectivity.

4 Conclusions

The preparation of CuZnO with different methods resulted in a significant modification in the structure and then led to the difference of the catalytic performance for the syngas hydrogenation at low temperature in liquid phase. The characterizations indicated that the preparation method had a substantial effect on the interaction between Cu and Zn to control the crystal particle growth and then led to the difference of the CO adsorption property. The precipitation method prepared CuZnO showed strong interaction between Cu and Zn, resulting in the low crystallinity and favoring the weak CO adsorption, while the sol gel prepared CuZnO showed weak interaction between Cu and Zn, resulting in the high crystallinity and promoting the strong CO adsorption. The crystallinity of CuZnO samples prepared by different method was sol gel > co precipitation > homogeneous precipitation. The results of the catalytic performances of CuZnO samples prepared by different methods showed that the order of the catalytic activity was homogeneous precipitation > co precipitation > sol gel, the order of the methanol selectivity was homogeneous precipitation > co precipitation > sol gel, and the order of the selectivity towards ethanol was sol gel > co precipitation > homogeneous precipitation, respectively. Meanwhile, the total carbon conversion was associated with the total amount of CO adsorption, the selectivity of methanol was linearly related with the amount of the weak CO adsorption, and the selectivity of ethanol was linearly related with the amount of the strong CO adsorption. It was found that low crystallinity was advantageous to the enhancement of the catalytic activity for the methanol synthesis, while high crystallinity decreased the catalytic

activity, but favored the strong CO adsorption for the growth of carbon chain to promote the ethanol synthesis.

Compliance with Ethical Standards

Conflict of interest The authors declare no conflict of interest.

References

- Spivey JJ, Egbibia A (2007) Heterogeneous catalytic synthesis of ethanol from biomass-derived syngas. *Chem Soc Rev* 36:1514–1528
- Wang F, Liu YW, Gan YH, Ding W, Fang WP, Yang YQ (2013) Study on the modification of Cu-based catalysts with cupric silicate for methanol synthesis from synthesis gas. *Fuel Process Technol* 110:190–196
- Deluga GA, Salge JR, Schmidt LD (2004) Renewable hydrogen from ethanol by autothermal reforming. *Science* 303:993–997
- Jorge MB, Anne GC, Andrei YK (2014) Effects of metal promotion on the performance of CuZnAl catalysts for alcohol synthesis. *ChemCatChem* 6:1788–1793
- Lu YW, Yu F, Hu J, Liu J (2012) Catalytic conversion of syngas to mixed alcohols over Zn-Mn promoted Cu-Fe based catalyst. *Appl Catal A* 429:48–58
- Lin M, Fang K, Li D, Sun Y (2008) CO hydrogenation to mixed alcohols over co-precipitated Cu-Fe catalysts. *Catal Commun* 9:1869–1873
- Subramani V, Gangwal SK (2008) A review of recent literature to search for an efficient catalytic process for the conversion of syngas to ethanol. *Energy Fuel* 22:814–839
- Mo XH, Tsai YT, Gao J, Mao DS, James GGG (2012) Effect of component interaction on the activity of Co/CuZnO for CO hydrogenation. *J Catal* 285:208–215
- Surisetty VR, Dalai AK, Kozinski J (2011) Alcohols as alternative fuels: an overview. *Appl Catal A* 404:1–11
- Sun J, Cai QX, Wan Y, Wan SL, Wang L, Lin JD, Mei DH, Wang Y (2016) Promotional effects of cesium promoter on higher alcohol synthesis from syngas over cesium-promoted Cu/ZnO/Al₂O₃ catalysts. *ACS Catal* 6:5771–5785
- Wang N, Fang K, Jiang D, Li D, Sun Y (2010) Iron carbide promoted K/β-Mo₂C for higher alcohols synthesis. *Catal Today* 158:241–245
- Christensen JM, Mortensen PM, Trane R, Jensen PA, Jensen AD (2009) Effects of H₂S and process conditions in the synthesis of mixed alcohols from syngas over alkali promoted cobalt-molybdenum sulfide. *Appl Catal A* 366:29–43
- Liu GL, Niu T, Cao A, Geng YX, Zhang Y, Liu Y (2016) The deactivation of Cu-Co alloy nanoparticles supported on ZrO₂ for higher alcohols synthesis from syngas. *Fuel* 176:1–10
- An Z, Ning X, He J (2017) Ga-promoted CO insertion and C-C coupling on Co catalysts for the synthesis of ethanol and higher alcohols from syngas. *J Catal* 356:157–164
- Ding MY, Ma LL, Zhang Q, Wang CG, Zhang WN, Wang TJ (2017) Enhancement of conversion from bio-syngas to higher alcohols fuels over K-promoted Cu-Fe bimodal pore catalysts. *Fuel Process Technol* 159:436–441
- Tsubaki N, Zeng JQ, Yoneyama Y, Fujimoto K (2001) Continuous synthesis process of methanol at low temperature from syngas using alcohol promoters. *Catal Commun* 2:213–217
- Graaf GH, Sijtsma P, Stambhuis EJ, Oostem G (1986) Chemical equilibria in methanol synthesis. *Chem Eng Sci* 41:2883–2890

18. Zeng JQ, Fujimoto K, Tsubaki N (2002) A new low-temperature synthesis route of methanol: catalytic effect of the alcoholic solvent. *Energy Fuel* 16:83–86
19. Herman RG, Smimmons GW, Klier K (1981) Catalytic synthesis of methanol from CO/H₂: III: the role of alumina and ceria in the Cu/ZnO system. *Stud Surf Sci Catal* 7:475–489
20. Ahoba-Sam C, Olsbye U, Jens KJ (2018) Low temperature methanol synthesis catalyzed by copper nanoparticles. *Catal Today* 299:112–119
21. Zhang K, Song HS, Sun DK, Li SF, Yang XG, Zhao YL, Huang Z, Wu YT (2003) Low-temperature methanol synthesis in a circulating slurry bubble reactor. *Fuel* 82:233–239
22. Reubroycharoen P, Vitidsant T, Yoneyama Y, Tsubaki N (2004) Development of a new low-temperature methanol synthesis process. *Catal Today* 89:447–454
23. Fan RG, Kyodo M, Tan L, Peng XB, Yang GH, Yoneyama Y, Yang RQ, Zhang QD, Tsubaki N (2017) Preparation and application of Cu/ZnO catalyst by urea hydrolysis method for low-temperature methanol synthesis from syngas. *Fuel Process Technol* 167:69–77
24. Liu H, Chen T, Yang G, Wang GY (2017) Investigation of active center of Cu-based catalyst for low temperature methanol synthesis from syngas in liquid phase: the contribution of Cu⁺ and Cu⁰. *Chemistryselect* 2:8000–8007
25. Tsubaki N, Ito M, Fujimoto K (2001) A new method of low-temperature methanol synthesis. *J Catal* 197:224–227
26. Ohyama S (2003) Low-temperature methanol synthesis in catalytic systems composed of copper-based oxides and alkali alkoxides in liquid media: effects of reaction variables on catalytic performance. *Topics Catal* 22:337–343
27. Lee ES, Aika K (1999) Low-temperature methanol synthesis in liquid-phase with a Raney Nickel-alkoxide system: effect of Raney Nickel pretreatment and reaction conditions. *J Mol Catal A* 141:241–248
28. Palekar VM, Jung H, Tierney JW, Wender I (1993) Alkali compounds and copper chromite as low-temperature slurry phase methanol catalysts. *Appl Catal A* 103:105–122
29. Yang R, Fu Y, Zhang Y, Tsubaki N (2004) In situ DRIFT study of low-temperature methanol synthesis mechanism on Cu/ZnO catalysts from CO₂-containing syngas using ethanol promoter. *J Catal* 228:23–35
30. Chu W, Zhang T, He C, Tang Y (2002) Low-temperature methanol synthesis (LTMS) in liquid phase on novel copper-based catalysts. *Catal Lett* 79:129–132
31. Gormley RJ, Rao VHS, Soong Y, Micheli E (1992) Methyl formate hydrogenolysis for low-temperature methanol synthesis. *Appl Catal A* 87:81–101
32. Zhao TS, Zhang K, Chen XR, Ma QX, Tsubaki N (2010) A novel low-temperature methanol synthesis method from CO/H₂/CO₂ based on the synergistic effect between solid catalyst and homogeneous catalyst. *Catal Today* 149:98–104
33. Yang RQ, Zhang Y, Iwama Y, Tsubaki N (2005) Mechanistic study of a new low-temperature methanol synthesis on Cu/MgO catalysts. *Appl Catal A* 288:126–133
34. Choi Y, Futagami K, Fujitani T, Nakamura J (2001) The role of ZnO in Cu/ZnO methanol synthesis catalysts-morphology effect or active site model. *Appl Catal A* 208:163–167
35. Fujitani T, Nakamura J (1998) The effect of ZnO in methanol synthesis catalysts on Cu dispersion and the specific activity. *Catal Lett* 56:119–124
36. Grunwaldt JD, Molenbroek AM, Topsoe NY, Clausen BS (2000) In situ investigations of structural changes in Cu/ZnO catalysts. *J Catal* 194:452–460
37. Behrens M, Studt F, Kasatkin I, Kuhl S, Hecker M, Abild-Pedersen F, Zander S, Girgsdies F, Kurr P, Knief BL, Tovar M, Fischer RW, Norskov JK, Schlögl R (2012) The active site of methanol synthesis over Cu/ZnO/Al₂O₃ industrial catalysts. *Science* 336:893–897
38. Nakamura J, Nakamura I, Uchijima T, Kanai Y, Watanabe T, Saito N, Fujitani T (1996) A surface science investigation of methanol synthesis over a Zn-deposited polycrystalline Cu surface. *J Catal* 160:65–67
39. Greeley J, Gokhale AA, Kreuser J, Dumesic JA, Topsoe H, Topsoe NY, Mavrikakis M (2003) CO vibrational frequencies on methanol synthesis catalysts: a DFT study. *J Catal* 213:63–72
40. Poels EK, Brands DS (2000) Modification of Cu/ZnO/SiO₂ catalysts by high temperature reduction. *Appl Catal A* 191:83–96
41. Johnston P, Hutchings GJ, Coville NJ, Finch KP, Moss JR (1999) CO hydrogenation using supported iron carbonyl complexes. *Appl Catal A* 186:245–253
42. Herman RG (2000) Advances in catalytic synthesis and utilization of higher alcohols. *Catal Today* 55:233–245
43. Mahdavi V, Peyrovi MH (2006) Synthesis of C1-C6 alcohols over copper/cobalt catalysts: investigation of the influence of preparative procedures on the activity and selectivity of Cu-Co₂O₃/ZnO, Al₂O₃ catalyst. *Catal Commun* 7:542–549
44. Tien-Thao N, Zahedi-Niaki MH, Alamdari H, Kaliaguine S (2007) Conversion of syngas to higher alcohols over nanosized LaCo_{0.7}Cu_{0.3}O₃ perovskite precursors. *Appl Catal A* 326:152–163
45. Chapelle A, Yaacob MH, Pasquet I, Presmanes L, Barnabe A, Tailhades P, Plessis JD, Kalantar-zadeh K (2011) Structural and gas-sensing properties of CuO-Cu_xFe_{3-x}O₄ nanostructured thin films. *Sens Actuator B* 153(1):117–124
46. Velu S, Suzuki K, Gopinath CS, Yoshida H, Hattori T (2002) XPS, XANES and EXAFS investigations of CuO/ZnO/Al₂O₃/ZrO₂ mixed oxide catalysts. *Phys Chem Chem Phys* 4:1990–1999
47. Wallbank B, Main IG, Johnson CE (1974) 2p and 2s shake-up satellites in solid compounds of 3d ions. *J Electron Spectrosc* 5:259–266
48. Kim KS (1974) Charge transfer transition accompanying X-ray photoionization in transition-metal compounds. *J Electron Spectrosc* 3:217–226
49. Mulligan RF, Iliadis AA, Kofinas P (2003) Synthesis and characterization of ZnO nanostructures templated using diblock copolymers. *J Appl Polym Sci* 89:1058–1061
50. Liang MS, Kang WK, Xie KC (2009) Comparison of reduction behavior of Fe₂O₃, ZnO and ZnFe₂O₄ by TPR technique. *J Nat Gas Chem* 18:110–113
51. Melian-Cabrera I, Lopez Granados M, Fierro JLG (2002) Pd-modified Cu-Zn catalysts for methanol synthesis from CO₂/H₂ mixtures: catalytic structures and performance. *J Catal* 210:285–294
52. Guo HJ, Li SG, Peng F, Zhang HR, Xiong L, Huang C, Wang C, Chen XD (2015) Roles investigation of promoters in K/Cu-Zn catalyst and higher alcohols synthesis from CO₂ hydrogenation over a novel two-stage bed catalyst combination system. *Catal Lett* 145:620–630
53. Kieger S, Delahay G, Coq B, Neveu B (1999) Selective catalytic reduction of nitric oxide by ammonia over Cu-FAU catalysts in oxygen-rich atmosphere. *J Catal* 183:267–280
54. Spencer MS (1999) The role of zinc oxide in Cu/ZnO catalysts for methanol synthesis and the water-gas shift reaction. *Top Catal* 8:259–266
55. van Herwijnen T, de Jong WA (1974) Brass formation in a copper/zinc oxide CO shift catalyst. *J Catal* 34:209–214

Affiliations

Huan Liu^{1,2} · Tong Chen¹ · Gongying Wang¹

✉ Tong Chen
chentongw@sina.com.cn

² University of Chinese Academy of Sciences, Beijing 100049,
People's Republic of China

¹ Chengdu Institute of Organic Chemistry, Chinese Academy
of Sciences, Chengdu 610041, People's Republic of China